

Corrosion behavior and mechanical properties of V-4Cr-4Ti alloy exposed at 500 and 700 °C to static Pb with $\sim 10^{-9}$ mass% dissolved oxygen for 1000 h

Valentyn Tsisar^{a,b,c,*}, Takuya Nagasaka^b, Olga Yeliseyeva^d, Jun Lim^c, Jürgen Konys^a, Takeo Muroga^b, Carsten Schroer^a

^a Karlsruhe Institute of Technology (KIT), Institute for Applied Materials – Applied Materials Physics (IAM-AWP), Hermann-von-Helmholtz-Platz 1, 76344 Eggenstein-Leopoldshafen, Germany

^b National Institute for Fusion Science (NIFS), Fusion Systems Research Division, Oroshi 322-6, Toki 509-5292, Japan

^c Belgian Nuclear Research Centre SCK•CEN, Boeretang 200, Mol B-2400, Belgium

^d Physical–Mechanical Institute of National Academy of Science of Ukraine, 5, Naukova Street, Lviv 79601, Ukraine

ABSTRACT

Keywords:
V-alloy
Liquid Pb
Corrosion

The corrosion tests of V-4Ti-4Cr alloy (NIFS HEAT 2) tensile samples were carried out in static liquid Pb with $\sim 10^{-9}$ mass% dissolved oxygen at 500 and 700 °C for 1000 h. A clear intergranular corrosion attack was observed on the surface of the samples. Corrosion losses increase ten times, from around 3.0 μm to 30 μm , as the temperature increased from 500 °C to 700 °C, respectively. The alloy remained ductile after the tests at both temperatures. A phenomenology of interaction processes in Pb[O]-V[Cr,Ti] system is discussed.

1. Introduction

Vanadium alloys are considered as potential materials for nuclear energy applications, both fusion and fission [1–4]. It is well known that the mechanical properties of V-alloys are very sensitive to non-metallic impurities (C, O, N, H) that exist in the initial alloy composition due to manufacturing or scavenging from surrounding gas or liquid metal (Li, Na) during operation [1,5–9].

In the V-alloy/liquid Li system, there is a transfer of oxygen from the solid metal to liquid Li, while carbon and nitrogen are scavenged by solid metal from the liquid Li [5,10]. In the V-alloy/liquid Na system, solid metal absorbs carbon and nitrogen, and is particularly sensitive to the concentration of oxygen in liquid sodium [5,10]. At low oxygen levels (2–6 ppm) in liquid sodium, V-alloys gained the weight in a protective manner. However, at high levels (10 ppm), the alloys lost weight, indicating corrosion [10]. Therefore, the importance of gettering liquid sodium to reduce oxygen content in order to enhance the corrosion resistance of V-alloys is underlined. The alloying elements, such as Cr, Mo, Fe, Ta, and Nb, reduce the solubility of oxygen in solid alloys, whereas Ti, Al and Zr enhance the level of oxygen absorption by the alloy [10]. Borgstedt summarized the research on sodium corrosion

of vanadium alloys and proposed that adequate corrosion resistance can only be achieved in V-alloys containing Cr and Ti in liquid metal with oxygen levels below 1×10^{-4} mass% by means of hot trapping with Zr [11].

The impetus for this study stems from the limited literature data on the compatibility of vanadium and V-alloys with Pb-based melts, although the V-alloys can be a promising alternative to steels, particularly at elevated temperatures (≥ 500 °C). The limited experimental and theoretical data on the corrosion behavior of vanadium and V-alloys in Pb-based molten metals are briefly reviewed below.

Ali-Khan carried out experiments on vanadium samples in a thermal convection loop at 625 °C for a duration of 1658 h and found no signs of corrosion [12]. Likewise, no corrosion was observed in vanadium samples when tested in circulating molten lead at 700 °C for 306 h. Furthermore, when tested in stationary lead up to approximately 950 °C, the vanadium samples indicated no signs of corrosion [12]. However, the waviness of the sample surface indicated potential vanadium dissolution at 950 °C for 100 h [13]. Subsequently, a noteworthy corrosion attack near the surface was observed after 20 h at 1100 °C [13].

Intermetallic compound formation was observed in the solid V/

* Corresponding author.

E-mail address: valentyn.tsisar@sckcen.be (V. Tsisar).

liquid Pb system after 400 h at 1000 °C, indicating corrosion interaction [14,15]. Smith notes that few reports exist on the relevant phase relationships in the V-Pb system [16], and some studies failed to synthesize the V₃Pb phase even at elevated temperatures and high pressures.

The solubility data calculations suggest that the maximum amount of V that can dissolve in Pb-based melts is only slightly less than that of Ni, which is known to be highly soluble [17]. This discovery is somewhat unexpected and contradicts the previously reported low solubilities of refractory metals in group V and VI within liquid metals [18].

Experimental data on corrosion interaction in the V, V-alloys/liquid Pb-Li system are available in the literature. These data are comparable to the corrosion interaction in Pb with low dissolved oxygen content, due to the high oxygen affinity of Li. Generally, the dissolution rates of V and V-alloys in Pb-Li are substantially lower when compared with austenitic and ferritic steels [19–21]. The scoping tests carried out in the Pb-17Li forced circulation loop at 430 °C for 2300 h revealed no measurable corrosion on V-15Cr-5Ti alloy [18]. In flowing Pb-17Li at 550 °C, however, samples of V-3Ti-1Si and V-15Cr-5Ti alloys showed some weight gain over time [22]. The weight gain was attributed to the Fe depositions, as a result of mass transfer from the material of the loop, while the samples themselves did not show any remarkable corrosion effect. At 830 K, mass transfer of Cr and Ni to the surface of the V-3Ti-1Si alloy was observed after 1000 h of exposure to flowing Pb-17Li, in addition to Fe [23]. The micro-hardness measurements revealed a hardened layer with a thickness of around 55 µm, indicating the uptake of non-metallic impurities by the alloy [22].

Regarding the influence of non-metallic impurities, it is expected that the V-alloy/liquid Pb system will exhibit similar behavior as the V-alloy/liquid Na system. Specifically, oxygen, which is the main non-metallic impurity in the liquid Pb, should be absorbed by the solid V-alloy.

In Pb and Pb-Bi eutectic, the oxygen concentration is maintained at certain level, typically between 10⁻⁷ and 10⁻⁶ mass% within the temperature range of 400 to 650 °C, in order to provide steel oxidation and prevent steel dissolution. At these concentrations, vanadium and V-alloys are expected to act as getters for oxygen dissolved in liquid Pb or Pb-Bi. However, the kinetics of the interaction is not investigated in order to draw a definitive conclusion regarding the potential degradation (embrittlement) of mechanical properties of V-alloys due to the uptake of oxygen from the liquid metal.

The aim of this work is to acquire preliminary data on the compatibility of the V-4Ti-4Cr alloy (NIFS HEAT 2) with liquid lead at high temperatures. The main objective is to perform the screening corrosion tests in static liquid lead with monitored concentration of dissolved oxygen at 500 and 700 °C and to determine the effect of 1000 h exposure on the corrosion and post-test mechanical properties of alloy.

2. Material and method

The V-4Ti-4Cr alloy NIFS-HEAT-2 (NH2) after solution annealing at 1273 K for 1 h is investigated in this work. Compared to similar alloys [2, 24], it is distinguished by its significantly lower non-metallic impurity

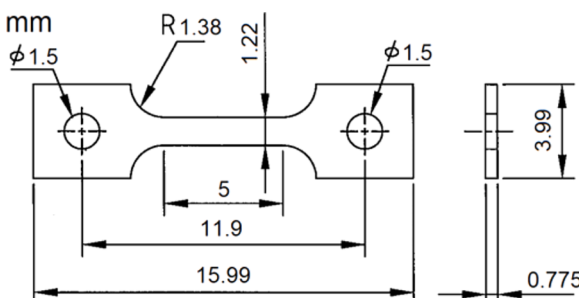


Fig. 1. Dimensions of V-4Ti-4Cr alloy tensile samples.

content (ppm%: 62C-84N-158O).

Tensile samples (15.99 × 1.22 × 0.775 mm) were machined (Fig.1) followed by additional degasation treatment in high vacuum (10⁻⁶ torr) at 400 °C for 1 h [25].

The apparatus for corrosion test is shown schematically in Fig.2. It consists of stainless steel capsule ended with a lid housing ports for: gas inlet and outlet; thermocouples residing in alumina tubes; an electrode (molybdenum wire) that closes the electric circuit; specimen holder (molybdenum rod); and two electrochemical oxygen sensors with a Pt/air reference electrode for active monitoring and controlling the oxygen concentration in the liquid lead [26]. The alumina crucible, filled with 2 kg of fresh lead, is positioned at the bottom of the steel capsule. The latter is placed in the vertical furnace (Fig.2). Working gasses (Ar, Ar-5vol%H₂, and synthetic air) are supplied over the surface of liquid metal by the Oxygen Control System (OCS) developed at Karlsruhe Institute of Technology (KIT) in order to provide the required oxygen concentration in the liquid metal.

Target conditions of corrosion tests are: 500 and 700 °C; 1000 h and “low” oxygen concentration in liquid Pb. The latter parameter was achieved by purging the Ar-5 vol% H₂ gas mixture over the surface of the liquid metal during the course of the test in order to minimize the oxygen content in liquid metal and its mass exchange from the liquid metal towards alloy.

When the output of sensor 1 (S1), which is placed at the level of samples, reaches the stable value, holder with samples is inserted into the liquid metal through the tube port (Fig.2). Sensor output was recalculated into the concentration of oxygen in the Pb using following equation [26]:

$$\log C_O(\text{mass}\%) = 2.3335 + \frac{6338.1}{T(K)} - 10,080 \frac{E^*(V)}{T(K)}$$

where: C_O – concentration of oxygen in Pb (mass%); $E^* = U - U_{th}$; U – sensor output (V); U_{th} – thermoelectric voltage resulting from different electric leads (V) and T – temperature (K).

Corrosion test at ~502(±0.5) °C was performed at constant concentration of oxygen measured at the level of samples (Sensor 1) of ~6 × 10⁻¹⁰ mass%O (Fig.3a). Concentration of oxygen at the top of the liquid metal surface which directly contacting covering gas Ar-5 vol% H₂ (Sensor 2) was higher ~8 × 10⁻⁹ mass%O at the same temperature ~501 (±0.5) °C.

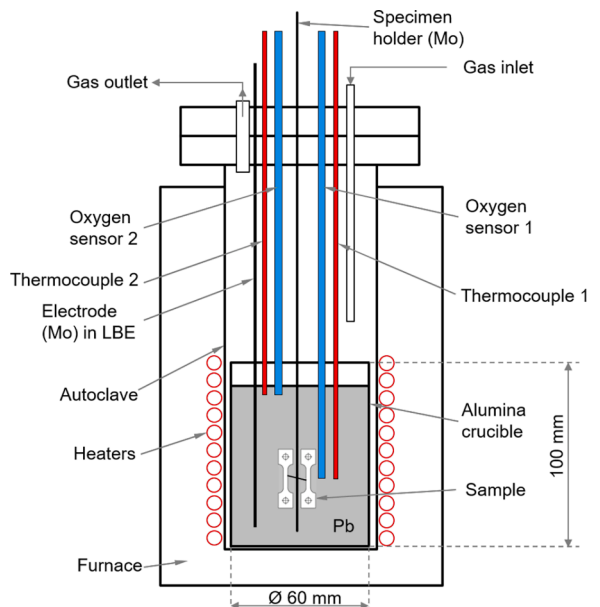


Fig. 2. Sketch of apparatus for corrosion test.

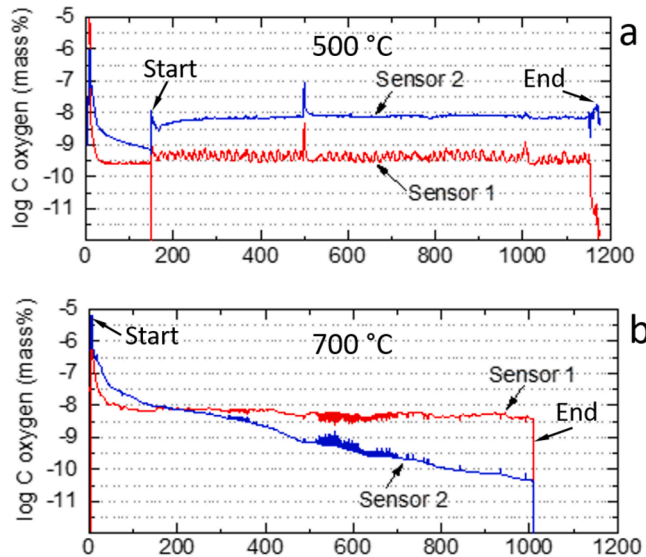


Fig. 3. Time dependence of oxygen concentration in liquid Pb during the exposure at 500 °C (a) and 700 °C (b).

Corrosion test at 701(± 2) °C was performed at concentration of oxygen measured at the level of samples (Sensor 1) of $\sim 8 \times 10^{-9}$ mass%O (Fig. 3b). Concentration of oxygen at the top of the liquid metal surface gradually decreased during the course of the test (Sensor 2) from about 10^{-6} to $\sim 6 \times 10^{-11}$ mass%O.

Based on the thermodynamic evaluations shown in Fig. 4 the concentration of the oxygen at both test temperatures was sufficiently enough in order to provide formation of the majority of vanadium oxides as well as Ti and Cr oxides.

Corrosion losses were determined by means of weight change measurements recalculated into the uniform thinning of sample using density of vanadium (6.1 g/cm³) and by direct measurements of post-test thickness of samples.

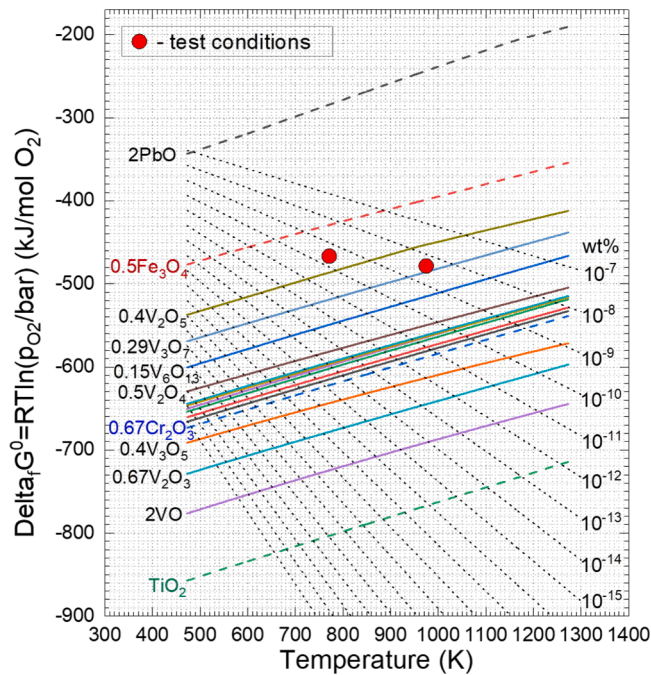


Fig. 4. Standard Gibbs free energy of formation ($\Delta_f G^0$) of vanadium oxides, in comparison with PbO, Fe₃O₄, Cr₂O₃, TiO₂ and concentrations (wt%) of oxygen dissolved in the liquid Pb depending on temperature (K).

Mechanical properties of the samples were determined using Slow Strain Rate Tensile (SSRT) test at room temperature and temperatures of tests (500 and 700 °C) with an initial strain rate 6.7×10^{-4} s⁻¹ and compared with those of the samples treated by standard vacuum annealing (VA). Vickers hardness was measured under the loading of 50 gf for 30 s. The Scanning Electron Microscope (SEM) equipped with Energy Dispersive X-ray (EDX) detector was used in order to determine morphological and compositional changes caused by the corrosion. Thermo Fisher Scios, which combines the FEG-SEM with a 30 kV Ga⁺ ion beam (Dual-Beam focused ion beam: DB-FIB) was used to mill local cross-sections directly from the samples surface areas of interest.

3. Results

In this paragraph, the results on corrosion behavior and post-test mechanical properties of the V-4Ti-4Cr alloy are presented.

3.1. Corrosion behavior

After corrosion tests, the surface of the samples was entirely covered by the well adhered and solidified lead. Thus, the samples were chemically cleaned in CH₃COOH-H₂O₂-C₂H₅OH (1:1:1) mixture at ~ 5 °C in order to remove adhered Pb. The cleaning procedure was repeated with a refreshed cleaning mixture until the weight of samples showed no change. After the intermediate cleaning step, which involved removing an adhered layer of shiny lead, a black-colored surface layer composed of V, Pb and O was observed according to the EDX surface analyses (Fig. 5). Following the final cleaning step, the black-colored corrosion layer disappeared, revealing a matte metallic surface on the samples. After the samples were cleaned, they were additionally degassed in a vacuum at 400 °C for one hour in order to remove hydrogen that may have been absorbed by the samples during cleaning, which could potentially affect the mechanical properties of alloy [25,27].

Fig. 6 shows morphology of corroded surface (a) and sub-surface zones (b, c) formed on the V-4Ti-4Cr sample after exposure at 500 °C to static liquid Pb for 1000 h. The sample revealed clear evidence of preferential intergranular corrosion attack. The surface of the grains facing the liquid lead is covered with small cavities (Fig. 6a,b). The corrosion losses illustrated in Fig. 7 show that in the average about 3 μ m were removed by the corrosion after 1000 h at 500 °C. The depth of intergranular attack, as shown in the representative example in Fig. 6c, reaches about 10 μ m, which is several times higher than the average corrosion attack. However, it does not exceed the grain size of the V-alloy (15–20 μ m), at least under the given duration of the test.

The corrosion losses increase by approximately ten times, reaching

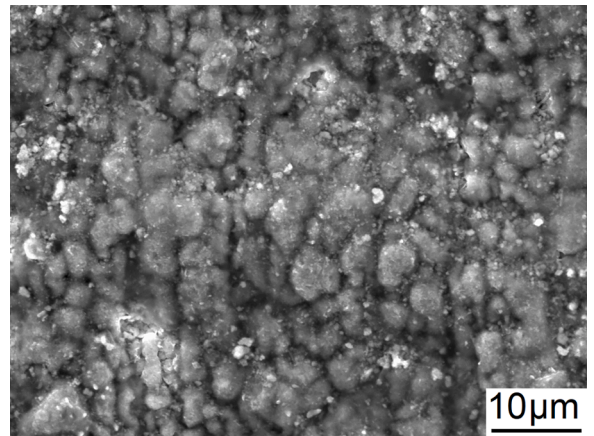


Fig. 5. Surface of corrosion layer covered samples after intermediate cleaning step when solidified Pb was removed revealing black-colored surface of corrosion layer.

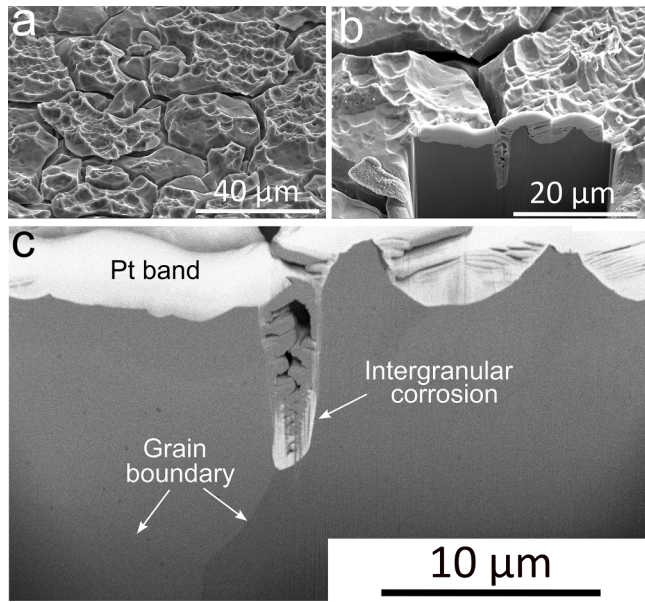


Fig. 6. Intergranular corrosion attack observed on the surface (a) and in the sub-surface zones (b, c) of V-4Ti-4Cr sample exposed at 500 °C to static liquid Pb for 1000 h.

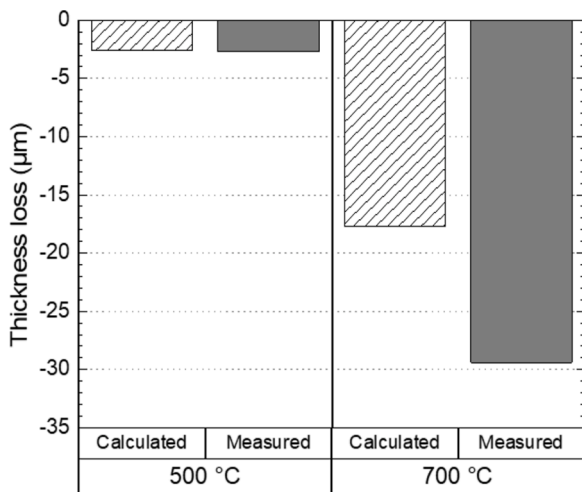


Fig. 7. Corrosion loss of samples exposed to static Pb at 500 and 700 °C for 1000 h.

about 30 μm, as the interaction test temperature increases from 500 to 700 °C (Fig.7). The grain boundaries and sub-structure of the grains experienced marked corrosion attack (Fig.8).

After the both tests, nevertheless, the composition of the corroded surfaces is identical to the initial composition of the alloy (wt%: V_{bal.} 4Ti-4Cr) based on the EDX analyses.

Two different types of Ti-rich precipitations were observed on the corroded surface of samples depending on the test temperature (Fig.9). Thus, after test carried out at 500 °C, the spherical precipitations were detected (Fig.9a,b), while after the test at 700 °C the plate-shaped precipitations were observed (Fig.9c,d). Similar plate-shaped precipitations were observed after the test performed at the same temperature (700 °C) and for similar time (1000 h) in liquid Li, and characterized as a Ti(CON) compounds [24,28].

Fig. 10 shows the scheme of developing of corrosion attack with respect to initial interface between solid alloy and liquid Pb. The very first near-surface row of grains experienced corrosion interaction during

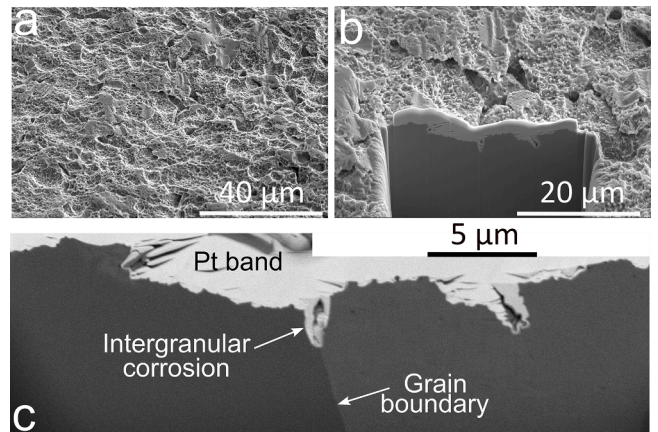


Fig. 8. Morphology of corroded surface (a) and sub-surface zones (b, c) of V-4Ti-4Cr sample exposed at 700 °C to static liquid Pb for 1000 h.

1000 h exposure of V-alloy at 500 °C. At 700 °C, at least two rows of grains have already undergone corrosion.

3.2. Mechanical properties

3.2.1. Hardness

The slight increase in hardness of the sample tested at 500 °C, compared to the unexposed sample, suggests that the alloy absorbed oxygen from the liquid metal (Fig.11). The sample exposed to liquid lead at 700 °C did not experienced any changes in hardness compared to the initial sample, while the visible decrease in surface hardness is attributed to a lower density of material caused by intergranular corrosion.

3.2.2. Slow strain rate tensile (SSRT) test

Fig. 12 shows stress-strain curves plotted depending on the tensile test temperature and compares initial and corroded samples. Table 1 summarizes the results of the tensile tests.

The tensile properties of samples exposed to liquid lead at 500 °C are not significantly different from those of initial samples (Fig.12a,b; Table1). Exposed samples retained their strength and ductility. Insufficient increase in strength, accompanied with a decrease in total elongation of Pb-exposed sample in the room temperature SSRT test, may result from slight hardening due to oxygen uptake, which correlates with a slight increase in hardness (Fig.12).

The SSRT test at 500 °C indicates that thermal exposure to liquid lead for 1000 h at the same temperature does not have an impact on the amplitude of serrations (~12.5 MPa) observed in strain-stress curves of initial and exposed samples as a result of the interaction between the interstitials and dislocations (Fig.12b). This result indirectly implying the absence of any influence of 1000 h exposure to liquid lead at 500 °C on the phase-structural state of alloy.

SSRT tests of samples exposed to liquid lead at 700 °C show a degradation in strength while maintaining uniform elongation as compared to the initial samples (Fig.12c,d). The total elongation of the exposed sample remains high enough (~35 %) after an SSRT test at room temperature (Fig.12c), whereas after an SSRT test at 700 °C, the total elongation significantly increased compared to the initial sample (Fig.12d).

Fig. 13 compares the fracture surfaces obtained in SSRT tests of initial and Pb-exposed tensile samples. The samples after corrosion tests showed substantial necking formation, similar to the initial samples, and a ductile fracture mode with characteristic dimples.

4. Discussion

It is well known that the oxygen could be present as an interstitial

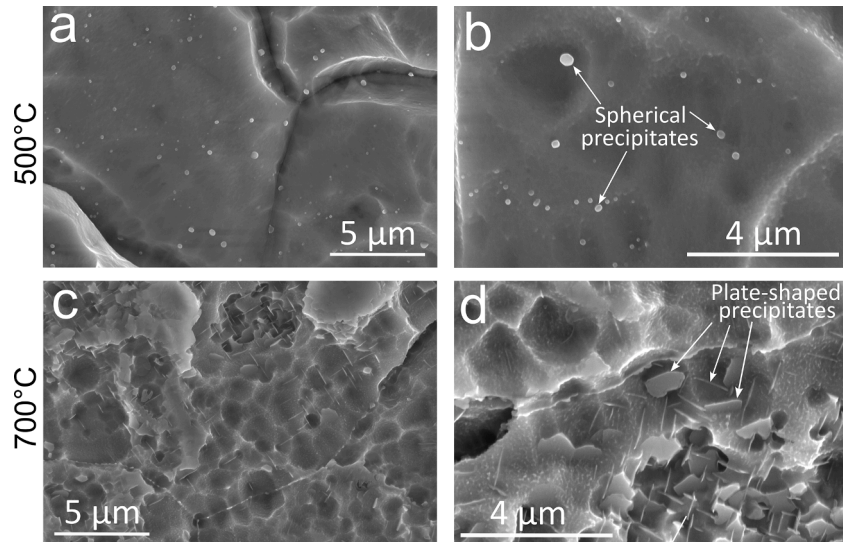


Fig. 9. Micrographs showing spherical (a, b) and plate-shaped (c, d) Ti-rich precipitations (Ti(CON)) observed in the composition of V-4Ti-4Cr alloy samples exposed at 500 °C (a, b) and 700 °C (c, d) to static liquid Pb for 1000 h.

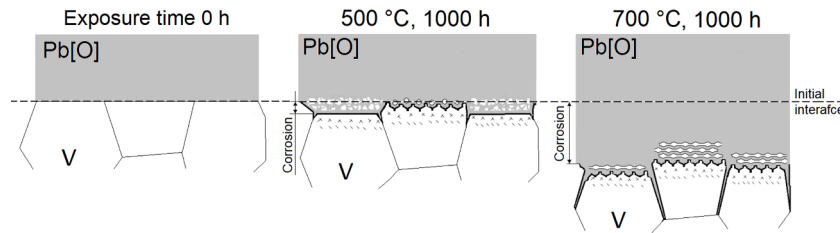


Fig. 10. The scheme of corrosion recession of V-alloy after 1000 h exposure to static liquid Pb at 500 and 700 °C.

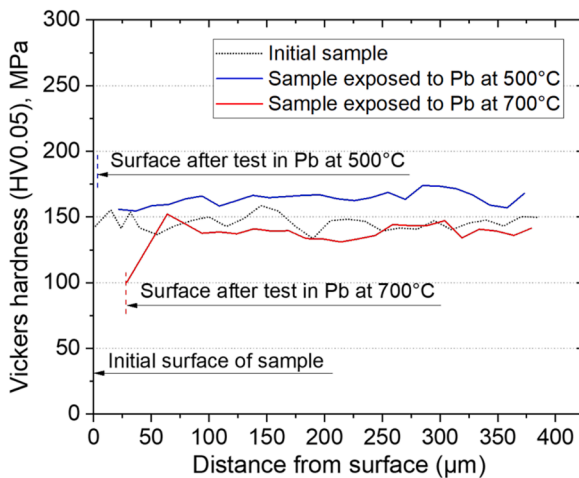


Fig. 11. Vickers hardness measured on the cross-section of initial sample and samples exposed to static Pb at 500 and 700 °C for 1000 h.

solute in the solid solution of vanadium BCC lattice and in the view of Ti (CON) precipitations [29]. In both cases, the strengthening of alloy takes place. The annealing at 1373 K, which dissolves precipitates, and subsequent reheating in the temperature range 873–973 K results in the reprecipitation strengthening of the V-4Ti-4Cr alloy [29]. In our work, V-alloy specimens were solution annealed at 1273 K prior to corrosion testing. Therefore, the subsequent corrosion exposure (aging) could affect the distribution of oxygen in vanadium matrix.

It seems that the test carried out in liquid lead at 500 °C for 1000 h

does not affect the phase-structural state of the alloy. It agrees well with the literature statements that at temperatures ≤ 500 °C the diffusion mobility of Ti atoms is low enough to scavenge oxygen from the solid solution, although the mobility of the latter is sufficient at this temperature [30,31]. The dynamic strain aging, observed as serrated stress-strain curves in the SSRT test performed at 500 °C for corrosion-tested samples (Fig.12b), indirectly confirms the presence of oxygen as an interstitial in the solid solution, similar to the initial sample.

However, after the corrosion test carried out at 700 °C for 1000 h, a reduction in strength and total elongation was observed in the room temperature SSRT test. It could be explained by the thinning of the effective cross-section of samples caused by the corrosion attack. The absence of a yield drop and the marked increase in total elongation of the sample (TE=40.4 %) compared to the initial sample (TE=26.2 %) may indirectly indicate about changes in the bulk composition of the alloy regarding interstitials and Ti(CON) precipitations and represent effect of aging, while a direct observations of plate-type Ti-based precipitations confirms this supposition (Fig.9d). It is difficult to separate the effect of temperature aging from the effect of corrosion for correct interpretation of the changes in tensile properties of samples since we did not performed in parallel the aging test in high vacuum. However, the observed softening of the alloy after the corrosion test at 700 °C indirectly indicates that the primary cause of the softening was due to aging rather than the corrosive environment of Pb[O].

Literature data regarding the effect of thermal aging on the evolution of phase-structural state of V-alloys are discussed briefly below, which may help us to shed a light on the our results.

At temperatures ≥ 600 °C, titanium becomes diffusional mobile which results in the interaction with interstitial atoms of O followed by formation of Ti(CON) precipitations [30]. However, the strengthening

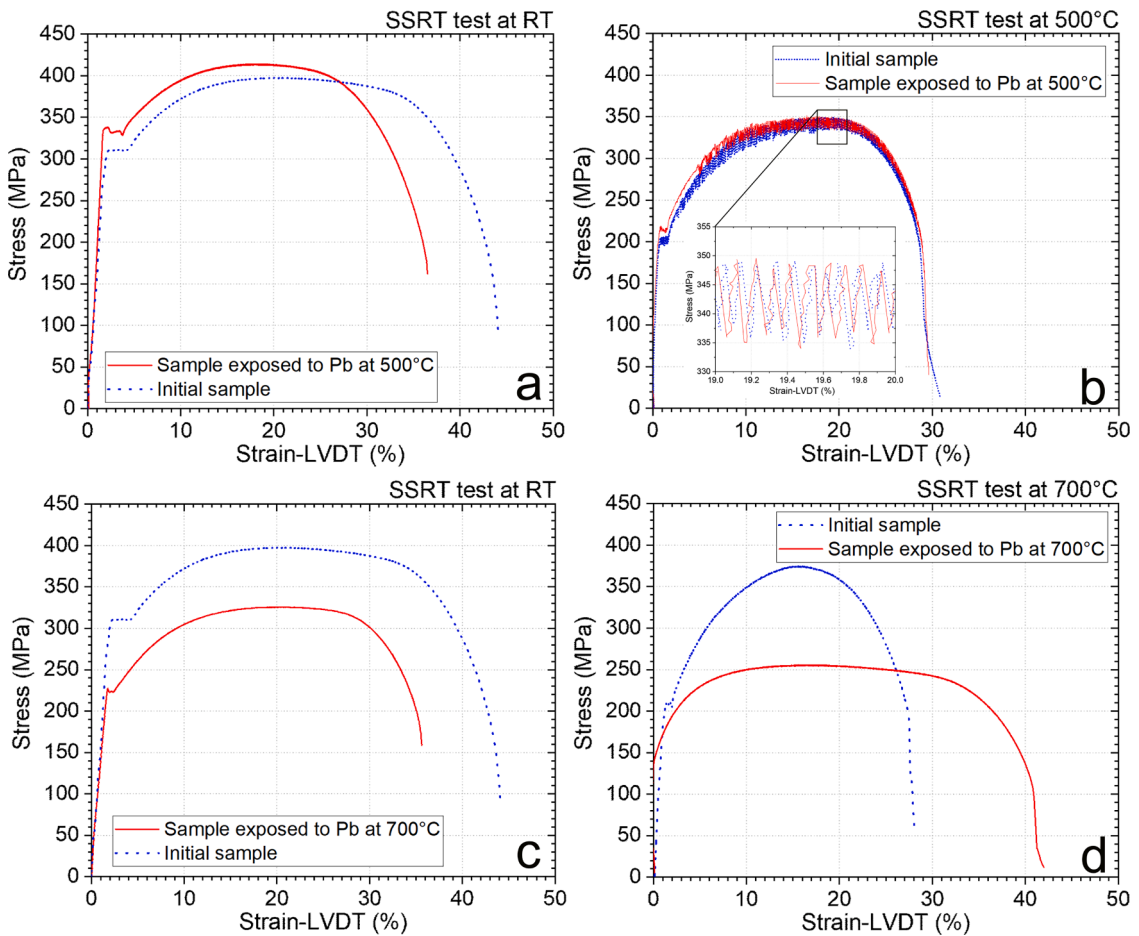


Fig.12. Stress – strain curves obtained by means of SSRT tests of initial samples (blue dotted lines) and samples exposed to static Pb (red solid lines) at 500 and 700 °C for 1000 h performed at room temperature (RT) (a, c) and 500 °C (b) and 700 °C (d).

Table 1

Tensile properties of initial samples and samples exposed to static Pb at 500 and 700 °C for 1000 h obtained by means of SSRT tests at room temperature and at 500 and 700 °C.

Exposure to Pb at temperature (°C)	Sample	SSRT test temperature (°C)	YS _{0.2}	UTS	UE	TE
			(MPa)	(MPa)	(%)	(%)
500	Initial	23	310.8	397.5	16.8	43.4
	Exposed to Pb	23	331.5	414.1	15.0	35.4
	Initial	500	208.7	349.7	16.1	30.9
	Exposed to Pb	500	232.0	351.7	13.9	29.4
700	Exposed to Pb	23	225.7	328.2	18.0	34.5
	Initial	700	209.0	374.6	12.7	26.2
	Exposed to Pb	700	185.1	255.7	13.7	40.4

effect disappears at temperatures > 700 °C because of precipitates coarsening [29]. Chen et al. studied the effect of aging at 600 °C for 393 h on the precipitation behavior and tensile properties of solution annealed V-alloys [32]. A significant peak in hardness ($\Delta HV53$) for the V-4Ti-4Cr alloy was observed after 10 h. Over time, however, the hardness gradually decreases and even after 393 h, it is still slightly higher ($\Delta HV20$) compared to the annealed state (HV146). A tensile test at room temperature shows an increase in strength properties similar to

the hardness tests, but elongation changes adversely with aging time [32].

Tensile properties of the V-4Cr-4Ti alloy degraded after exposure at 700 and 800 °C to liquid Li for up to 1443 h. Nonetheless, the alloy maintained good ductility despite substantial contamination by C and N from the liquid metal [33]. The 80 MPa decrease in ultimate tensile strength (UTS) after the exposure at 800 °C to liquid Li in SSRT tests carried out at 700 and 800 °C was supposed to be attributed to several possible mechanisms: the loss of precipitation hardening caused by Ti-C-O precipitates; the loss of hardening from oxygen in solid solution and changes in grain-boundary conditions.

Similar tests carried out in static liquid Li at 700 and 800 °C for 1000 h resulted in the increase in strength and a decrease in ductility of V-4Cr-4Ti alloy due to the uptake of nitrogen by the solid alloy from the liquid metal, followed by Ti₂CON precipitation hardening [28]. However, the ductility remained high even after a 1000 h exposure at 700 and 800 °C.

An increase in strength accompanied by the minor decrease in ductility and a reduced dynamic strain aging were observed in tensile tests performed in vacuum at 500 °C on samples of V-4Cr-4Ti alloy exposed to flowing Li (2–3 cm/s) with temperatures ranging from 400 to 700 °C for 2355 h [34]. However the near-surface layer with higher hardness and grain boundaries with increased number of Ti- and N-rich precipitates was formed. Samples aged at 700 °C in Ar-filled quartz ampoule for 2355 h showed no effect on the tensile properties of alloy.

Summarizing the effect of aging, it can be noted that the V-4Cr-4Ti alloy during the exposure at 700 °C to liquid lead for 1000 h goes relatively quickly through the stages of precipitation-assisted hardening followed by the softening, which is caused by the growth and

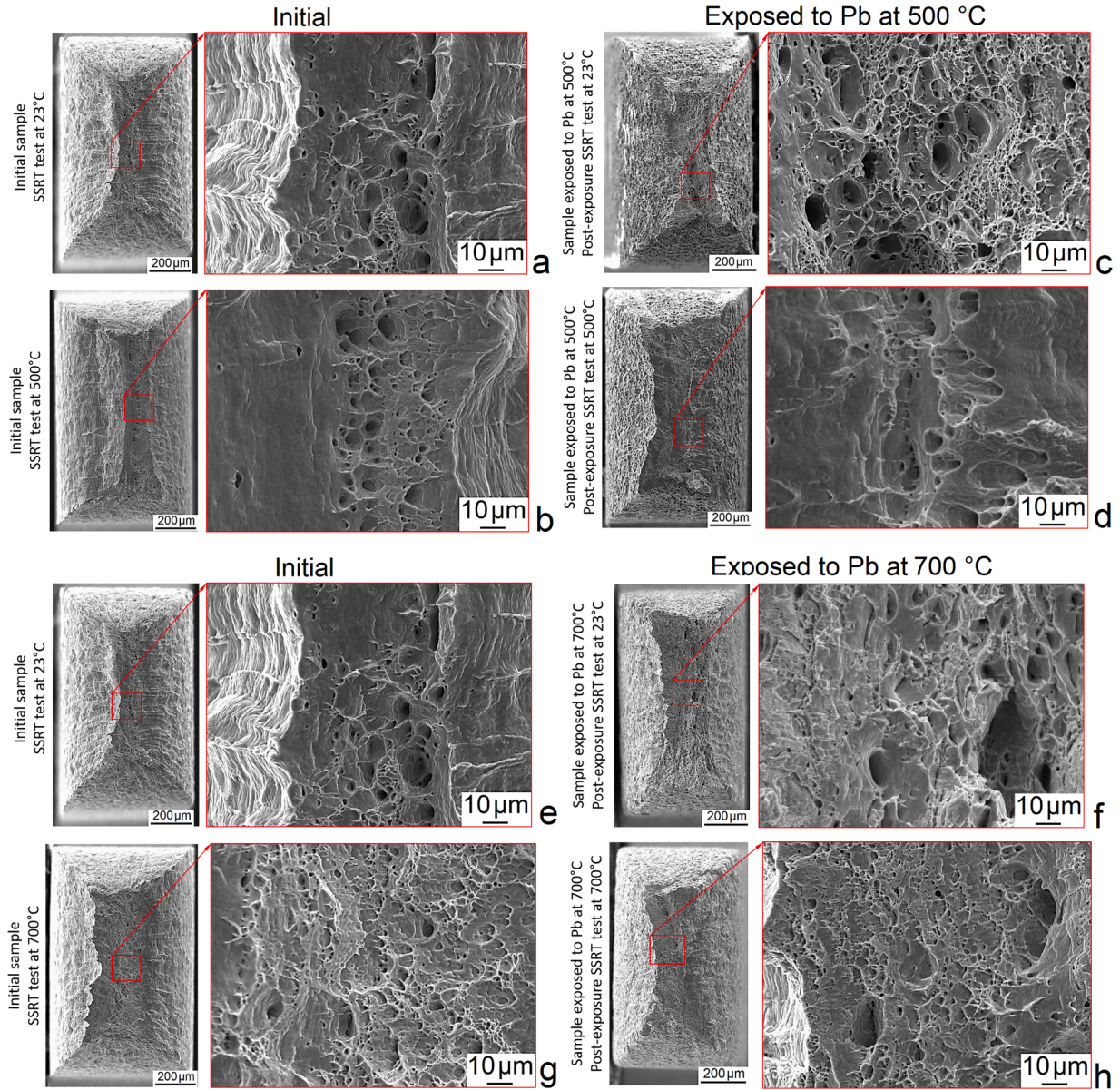


Fig. 13. Fracture surface of samples after SSRT test of initial samples (a, b, e, g) and samples exposed to static Pb at 500 °C (c, d) and 700 °C (f, h) for 1000 h, performed at room temperature (RT) (a, c, e, f), 500 °C (b, d) and 700 °C (g, h).

coagulation of Ti(CON) precipitations as a result of high diffusion mobility of Ti and interstitials in solid solution at this temperature.

Based on the obtained results a phenomenological interaction in solid V-alloy/liquid Pb[O] system could be described as the following steps: the interaction starts with oxygen diffusion from liquid lead towards the solid surface of the V-alloy as a result of differences in the chemical potential of oxygen in the liquid and solid phases. Oxygen atoms, adsorbed at the solid surface, diffuse further into the V-matrix which results in the formation of near-surface zone where oxygen is present in solid solution of V-alloy lattice as an interstitial. As the concentration of oxygen in solid solution increases with time and reaches solubility limit, the formation of V-O oxides (most probably VO) takes place in the vicinity of the solid metal/liquid metal interface. The formation of V-O oxide layer stimulates increase in oxygen activity at the side of the liquid metal, which in turn results in formation of Pb-O complexes. The latter could react with V-oxide surface layer with formation of triple oxide $Pb_xV_yO_z$, an existence of which is confirmed in phase diagram PbO - V_2O_5 [35]. It is worth mentioning that the corrosion products are growing at the expense of the vanadium matrix, i.e., from

the initial solid V-alloy/liquid Pb interface into the material bulk. The corrosion develops preferentially along the grain boundaries which are less stable against chemical attack [11].

The further experimental work is necessary in order to better understand the mechanisms of interaction in liquid Pb[O]/solid V-alloy system and determine the optimal temperature - oxygen concentration ranges in order to minimize the corrosion providing at the same time the long-term stability of mechanical properties, as well as to investigate susceptibility of V-alloys to liquid-metal embrittlement in lead-based melts as the material with a body centered cubic structure.

5. Conclusions

Screening tests on the corrosion compatibility between V-4Ti-4Cr alloy and static liquid Pb with $\sim 10^{-9}$ mass% dissolved oxygen at 500 and 700 °C for 1000 h were carried out. Based on the observed corrosion interaction and mechanical properties, the following conclusions can be drawn:

- The V-alloy experienced intergranular corrosion attack which accumulated in the near-surface zone and proceeded through the formation of non-protective $V_xPb_yO_z$ oxides;
- Average corrosion losses increase by a factor of ten, from 3.0 to 30 μm , as the interaction temperature increased from 500 to 700 $^{\circ}\text{C}$, respectively;
- The V-alloy retained ductility after 1000 h exposure at both test temperatures, although it lost strength at 700 $^{\circ}\text{C}$ due to aging;
- The V-alloys could be a good alternative to steels in liquid Pb with low oxygen concentration at high temperatures $500\text{ }^{\circ}\text{C} \leq T < 700\text{ }^{\circ}\text{C}$.

CRediT authorship contribution statement

Valentyn Tsisar: Visualization, Validation, Methodology, Investigation, Formal analysis, Data curation, Conceptualization, Writing – original draft. **Takuya Nagasaka:** Conceptualization, Data curation, Formal analysis, Funding acquisition, Methodology, Resources, Writing – review & editing. **Olga Yeliseyeva:** Conceptualization, Formal analysis, Validation, Visualization, Writing – original draft, Writing – review & editing. **Jun Lim:** Data curation, Formal analysis, Visualization, Writing – review & editing. **Jürgen Kony:** Formal analysis, Resources, Supervision, Writing – review & editing. **Takeo Muroga:** Resources, Supervision, Writing – review & editing. **Carsten Schroer:** Conceptualization, Data curation, Formal analysis, Methodology, Writing – review & editing.

Declaration of competing interest

The authors declare that they have no known competing financial interests or personal relationships that could have appeared to influence the work reported in this paper.

Data availability

The data that has been used is confidential.

Acknowledgments

The investigations are performed in the framework of in-kind collaboration initiative among the nuclear materials and corrosion groups of Karlsruhe Institute of Technology (KIT, Germany), National Institute for Fusion Science (NIFS, Japan), Belgian Nuclear Research centre (SCK•CEN, Belgium) and Physical–Mechanical Institute of National Academy of Science of Ukraine (PhMI NASU, Ukraine). The authors would like to thank for assistance in FEG-SEM to Ms. Lopes Maia Eloa (Vrije Universiteit Brussel, SCK.CEN).

References

- [1] T. Muroga, J.M. Chen, V.M. Chernov, R.J. Kurtz, M.L. Flem, Present status of vanadium alloys for fusion applications, *J. Nucl. Mater.* 455 (2014) 263–268, <https://doi.org/10.1016/j.jnucmat.2014.06.025>.
- [2] L.L. Sneed, D.T. Hoelzer, M. Rieth, A.A. Nemith, *Refractory alloys: vanadium, niobium, molybdenum, tungsten*, R. Odette, S. Zinkle (Eds.), *Structural Alloys For Nuclear Energy Applications*, Elsevier, Amsterdam, Amsterdam, Netherlands, Oxford, England, Cambridge, Massachusetts, 2019, pp. 585–640.
- [3] S. Zinkle, H. Matsui, D. Smith, A. Rowcliffe, E. van Osch, K. Abe, V. Kazakov, Research and development on vanadium alloys for fusion applications, *J. Nucl. Mater.* 258–263 (1998) 205–214, [https://doi.org/10.1016/S0022-3115\(98\)00269-4](https://doi.org/10.1016/S0022-3115(98)00269-4).
- [4] R.J. Kurtz, K. Abe, V.M. Chernov, V.A. Kazakov, G.E. Lucas, H. Matsui, T. Muroga, G.R. Odette, D.L. Smith, S.J. Zinkle, Critical issues and current status of vanadium alloys for fusion energy applications, *J. Nucl. Mater.* 283–287 (2000) 70–78, [https://doi.org/10.1016/S0022-3115\(00\)00351-2](https://doi.org/10.1016/S0022-3115(00)00351-2).
- [5] K. Natesan, Influence of nonmetallic elements on the compatibility of structural materials with liquid alkali metals, *J. Nucl. Mater.* 115 (1983) 251–262.
- [6] A. Nishimura, A. Iwahori, N. Heo, T. Nagasaka, T. Muroga, S.-I. Tanaka, Effect of precipitation and solution behavior of impurities on mechanical properties of low activation vanadium alloy, *J. Nucl. Mater.* 329–333 (2004) 438–441, <https://doi.org/10.1016/j.jnucmat.2004.04.072>.
- [7] J.M. Chen, T. Muroga, T. Nagasaka, Y. Xu, C. Li, S.Y. Qiu, Y. Chen, Precipitation behavior in V–6–4Ti, V–4Ti and V–4Cr–4Ti alloys, *J. Nucl. Mater.* 334 (2004) 159–165, <https://doi.org/10.1016/j.jnucmat.2004.05.019>.
- [8] Y. Wu, T. Muroga, Q. Huang, Y. Chen, T. Nagasaka, A. Sagara, Effects of impurities on low activation characteristics of V–4Cr–4Ti alloy, *J. Nucl. Mater.* 307–311 (2002) 1026–1030, [https://doi.org/10.1016/S0022-3115\(02\)01167-4](https://doi.org/10.1016/S0022-3115(02)01167-4).
- [9] T. Kainuma, N. Iwao, T. Suzuki, R. Watanabe, Effects of oxygen, nitrogen and carbon additions on the mechanical properties of vanadium and V/Mo alloys, 9th Int. Conf. Fusion Reactor Mater. 80 (1979) 339–347, [https://doi.org/10.1016/0022-3115\(79\)90197-1](https://doi.org/10.1016/0022-3115(79)90197-1).
- [10] R.L. Ammon, Vanadium and vanadium-alloy compatibility behaviour with lithium and sodium at elevated temperatures, *Int. Metals Rev.* 25 (1980) 255–268, <https://doi.org/10.1179/imtr.1980.25.1.255>.
- [11] H.U. Borgstedt, Influence of liquid sodium on mechanical properties of steels, refractory alloys and ceramics, in: Ghetta, V., Gorse, D., Maziere, D., Pontikis, V. (eds) *Materials Issues for Generation IV Systems*. NATO Science for Peace and Security Series B: Physics and Biophysics, Springer, Dordrecht, pp. 461–480.
- [12] I. Ali-Khan, Corrosion of steels and refractory metals in liquid lead, in: Borgstedt (Ed.) 1982 – Material behavior and Physical Chemistry in Liquid Metal Systems, pp. 243–252.
- [13] I. Ali Khan, *Berichte der Kernforschungsanlage Jülich Nr. 661*, 1970.
- [14] R.J. Cash, R.M. Fisher, M.R. Core, Compatibility studies of several molten uranium and thorium alloys in niobium, tantalum, and yttrium. Research and Development Report, Ames Laboratory at Iowa State University of Science and Technology, 1964.
- [15] W.D. Manly, Fundamentals of liquid metal corrosion, *Corrosion* 12 (1956) 46–52.
- [16] J.F. Smith, The Pb–V (Lead–Vanadium) system, *Bull. Alloy Phase Diag.* 2 (1981) 209–210, <https://doi.org/10.1007/BF02881481>.
- [17] G.M. Grazinov, V.A. Evtikhin, L.P. Zavialskiy, A.Y. Kosuhin, I.E. Lyblinskii, *Material Science of Liquid Metal Systems of Thermonuclear Reactors*, Energoatomizdat, Moscow, 1989.
- [18] O.K. Chopra, D.L. Smith, P.F. Tortorelli, J.H. DeVan, D.K. Sze, Liquid-metal corrosion, *Fusion Technol.* 8 (1985) 1956–1969, <https://doi.org/10.13182/FST85-A24572>.
- [19] H. Gräbner, H. Feuerstein, J. Oschinski, Compatibility of metals and alloys in liquid Pb–17Li at temperatures up to 650 $^{\circ}\text{C}$, 9th Int. Conf. Fusion Reactor Mater. 155–157 (1988) 702–704, [https://doi.org/10.1016/0022-3115\(88\)90399-6](https://doi.org/10.1016/0022-3115(88)90399-6).
- [20] *Challenges For Coolants in Fast Neutron Spectrum Systems*, International Atomic Energy Agency (IAEA), Vienna, 2020. IAEA-TECDOC-1912.
- [21] H. Feuerstein, H. Gräbner, J. Oschinski, S. Horn, Compatibility of refractory metals and beryllium with molten Pb17Li, *J. Nucl. Mater.* 233–237 (1996) 1383–1386, [https://doi.org/10.1016/S0022-3115\(96\)00192-4](https://doi.org/10.1016/S0022-3115(96)00192-4).
- [22] H.U. Borgstedt, M. Grundmann, J. Kony, Z. Perić, A vanadium alloy for the application in a liquid metal blanket of a fusion reactor, *J. Nucl. Mater.* 155–157 (1988) 690–693, [https://doi.org/10.1016/0022-3115\(88\)90396-0](https://doi.org/10.1016/0022-3115(88)90396-0).
- [23] C. Adelhelm, D. Kempf, E. Nold, Analysis of V–3Ti–1Si alloy after exposure to Pb–17Li, *J. Nucl. Mater.* 155–157 (1988) 698–701, [https://doi.org/10.1016/0022-3115\(88\)90398-4](https://doi.org/10.1016/0022-3115(88)90398-4).
- [24] N.J. Heo, T. Nagasaka, T. Muroga, Recrystallization and precipitation behavior of low-activation V–Cr–Ti alloys after cold rolling, *J. Nucl. Mater.* 325 (2004) 53–60, <https://doi.org/10.1016/j.jnucmat.2003.10.012>.
- [25] R.E. Buxbaum, D.L. Smith, J.-H. Park, Hydrogen solubility in V–4Cr–4Ti alloy, *J. Nucl. Mater.* 307–311 (2002) 576–579, [https://doi.org/10.1016/S0022-3115\(02\)01215-1](https://doi.org/10.1016/S0022-3115(02)01215-1).
- [26] C. Schroer, O. Wedemeyer, J. Kony, Aspects of minimizing steel corrosion in liquid lead-alloys by addition of oxygen, *Nucl. Eng. Des.* 241 (2011) 4913–4923, <https://doi.org/10.1016/j.jnucengdes.2011.09.002>.
- [27] V. Tisar, O. Yeliseyeva, T. Muroga, T. Nagasaka, Effect of lithium purity on in-situ formation of Er2O3 oxide layer on V–4Ti–4Cr Alloy, *Plasma Fusion Res.* 7 (2012) 2405123, <https://doi.org/10.1585/pfr.7.2405123>.
- [28] M. Li, D.T. Hoelzer, M.L. Grossbeck, The Influence of lithium environment on tensile behavior and microstructure of V–4Cr–4Ti, *J. Nucl. Mater.* 392 (2009) 364–370, <https://doi.org/10.1016/j.jnucmat.2009.03.026>.
- [29] T. Muroga, Vanadium for nuclear systems, in: R.J.M. Konings, T.R. Allen, R. E. Stoller, S. Yamanaka (Eds.), *Comprehensive Nuclear Materials*, Elsevier, Amsterdam, 2012, pp. 391–406.
- [30] D. Hoelzer, M. West, S. Zinkle, A. Rowcliffe, Solute interactions in pure vanadium and V–4Cr–4Ti alloy, *J. Nucl. Mater.* 283–287 (2000) 616–621, [https://doi.org/10.1016/S0022-3115\(00\)00344-5](https://doi.org/10.1016/S0022-3115(00)00344-5).
- [31] R.E. Gold, D.L. Harrod, R.L. Ammon, J.R.W. Buckman, R.C. Svedberg, Technical assessment of vanadium-base alloys for fusion reactor applications, in: *Review of properties: Vanadium and Vanadium-Base Alloys*, 2, 1978. Final report.
- [32] J.M. Chen, T. Muroga, T. Nagasaka, S.Y. Qiu, C. Li, Y. Chen, B. Liang, Z.Y. Xu, The mechanical properties of V–4Cr–4Ti in various thermo-mechanical states, *Fusion Eng. Des.* 81 (2006) 2899–2905, <https://doi.org/10.1016/j.fusengdes.2006.07.051>.
- [33] T. Nagasaka, T. Muroga, M. Li, D.T. Hoelzer, S.J. Zinkle, M.L. Grossbeck, H. Matsui, Tensile property of low activation vanadium alloy after liquid lithium exposure, *Fusion Eng. Des.* 81 (2006) 307–313, <https://doi.org/10.1016/j.fusengdes.2005.09.029>.
- [34] K.A. Unocic, M.J. Lance, B.A. Pint, Characterization of specimens exposed in a Li loop, *J. Nucl. Mater.* 442 (2013) S580–S584, <https://doi.org/10.1016/j.jnucmat.2013.04.055>.
- [35] W. Xie, N. Wang, Z. Qiao, Z. Cao, Thermodynamic assessment of the PbO–V2O5 system, *Calphad* 55 (2016) 41–46, <https://doi.org/10.1016/j.calphad.2016.04.005>.